Journal of Neurochemistry

JOURNAL OF NEUROCHEMISTRY | 2010 | 114 | 795–809 doi: 10.1111/j.1471-4159.2010.06806.x

AAV-mediated expression of wild-type and ALS-linked mutant VAPB selectively triggers death of motoneurons through a Ca^{2+}-dependent ER-associated pathway

Karine Langou,*,† Anice Moumen,*,† Christophe Pellegrino,†,‡ Julianne Aebischer*,† Igor Medina,†,‡ Patrick Aebischer§ and Cédric Raoul*,†

*Inserm-Avenir team, The Mediterranean Institute of Neurobiology, Marseille, France

†Université Aix-Marseille, Faculté des Sciences, Marseille, France

‡Inserm U901, the Mediterranean Institute of Neurobiology, Marseille, France

§Brain Mind Institute, Ecole Polytechnique Fédérale de Lausanne (EPFL), Lausanne, Switzerland

Abstract

A dominant mutation in the gene coding for the vesicle-associated membrane protein-associated protein B (VAPB) was associated with amyotrophic lateral sclerosis, a fatal paralytic disorder characterized by the selective loss of motoneurons in the brain and spinal cord. Adeno-associated viral vectors that we show to transduce up to 90% of motoneurons *in vitro* were used to model VAPB-associated neurodegenerative process. We observed that Adeno-associated viral-mediated over-expression of both wild-type and mutated form of human VAPB selectively induces death of primary motoneurons, albeit with different kinetics. We provide evidence that ER stress and impaired homeostatic regulation of calcium (Ca^{2+}) are implicated in the death process. Finally, we found that completion of the motoneuron death program triggered by the over-expression of wild-type and mutant VAPB implicates calpains, caspase 12 and 3. Our viral-based *in vitro* model, which recapitulates the selective vulnerability of motoneurons to the presence of mutant VAPB and also to VAPB gene dosage effect, identifies aberrant Ca^{2+} signals and ER-derived death pathways as important events in the motoneuron degenerative process.

Keywords: adeno-associated virus, amyotrophic lateral sclerosis, calcium, endoplasmic reticulum stress, motoneuron culture, vesicle-associated membrane protein-associated protein B.

J. Neurochem. (2010) **114**, 795–809.

Amyotrophic lateral sclerosis (ALS) is a progressive paralytic disorder that primarily affects motoneurons of the motor cortex, brainstem and spinal cord. ALS, which is largely sporadic, typically manifests in midlife, and death follows 3–5 years after onset. The disorder is characterized by muscle weakness that inexorably evolves into a generalized paralysis. Unfortunately a cure is not yet available (Meininger 2005; Van Damme and Robberecht 2009).

As the discovery of mutations in the superoxide dismutase-1 (SOD1) gene in familial cases (FALS), an increasing number of genes in which mutations cause FALS have been identified (Dion *et al.* 2009). From this genetic knowledge, experimental models that recapitulate the selective vulnerability of motoneurons have been successfully developed in mice and rats with SOD1 mutants (Turner and Talbot 2008). Recently mice expressing a TDP-43 mutant with some

Received March 16, 2010; revised manuscript received May 3, 2010; accepted May 3, 2010.

Address correspondence and reprint requests to Cédric Raoul, Inserm-Avenir team, The Mediterranean Institute of Neurobiology, Inmed. 163 Route de Luminy, Marseille, France. E-mail: cedric.raoul@inserm.fr

Abbreviations used: AAV, adeno-associated viral; ALS, amyotrophic lateral sclerosis; AMPA, α-amino-3-hydroxy-5-methylisoxazole-4-propionate; ATF6, activating transcription factor 6; BAPTA, 1,2-*bis*(2-Aminophenoxy)ethane-N,N,N',N'-tetraacetic acid; CICR, Ca^{2+}-induced Ca^{2+} release; DPI, day post-infection; EGFP, enhanced green fluorescent protein; ER, endoplasmic reticulum; FALS, familial ALS; IRE1, inositol-requiring enzyme 1; KA, kainate; m.o.i, multiplicity of infection; NBQX, 2,3-Dihydroxy-6-nitro-7-sulfamoyl-benzo (F) 9 quinoxaline; P56S, proline 56 to serine; PBS, phosphate-buffered saline; PGK1, phosphoglycerokinase; RyRs, ryanodine receptors; SOD1, superoxide dismutase-1; TU, transducing units; UPR, unfolded protein response; VAPA, vesicle-associated membrane protein-associated protein A; VAPB, VAP protein B; XBP1, X-box binding protein; z-ATAD-fmk, z-Ala-Thr-Ala-Asp(OME)-fmk.

features of ALS and frontotemporal lobar degeneration have been documented (Wegorzewska *et al.* 2009). Complementarily, primary, embryonic or induced pluripotent stem cell-based motoneuron cultures from SOD1 mutant mice or ALS patients are being regarded as a solid approach to gain insights into physio-pathological mechanisms of ALS (Raoul *et al.* 2006; Nagai *et al.* 2007; Dimos *et al.* 2008).

A dominantly inherited mutation in the gene encoding for the vesicle-associated membrane protein-associated protein B (VAPB) has been associated with typical ALS, atypical ALS and late-onset spinal muscular atrophy (Nishimura *et al.* 2004). VAPB is a ubiquitously expressed membrane-anchored protein that localizes mainly to the endoplasmic reticulum (ER) and ER-Golgi intermediate vesicles (Soussan *et al.* 1999; Lev *et al.* 2008). VAPB has been proposed to play a role in coat protein complex I-mediated retrograde transport of proteins (Soussan *et al.* 1999), lipid transfer toward the Golgi (Peretti *et al.* 2008), and also to regulate ER structure through interaction with the microtubule network (Amarilio *et al.* 2005; Prosser *et al.* 2008) or to modulate response to ER stress (Kanekura *et al.* 2006; Gkogkas *et al.* 2008; Suzuki *et al.* 2009). Studies in neuronal and non-neuronal cell lines showed that the proline 56 to serine (P56S) VAPB mutant forms dense cytosolic aggregates continuous with ER structures. These $VAPB^{P56S}$ inclusions may exert dominant negative effects by recruiting and insolubilizing the wild-type form of VAPB (Kanekura *et al.* 2006; Teuling *et al.* 2007; Suzuki *et al.* 2009). However, the impact of mutant VAPB on the functional integrity of motoneurons remains elusive.

Here, we report that adeno-associated viral (AAV) vector-mediated expression of both human wild-type and mutant VAPB selectively triggers death of embryonic motoneurons. We provide evidence that ER stress and an impaired calcium (Ca^{2+}) homeostasis participate in the death program initiated by wild-type or mutant VAPB over-expression. We demonstrate that the hVAPB-associated degenerative process occurs in a caspase-dependent manner in cultured motoneurons. We describe an *in vitro* model of VAPB-associated selective degeneration of motoneurons that provides evidence that Ca^{2+} signals associated to ER-derived pathways might contribute to the pathologic loss of motoneurons.

Materials and methods

Expression constructs

Coding sequences of hVAPB (Genbank NM004738) and human vesicle-associated membrane protein-associated protein A (hVAPA) (genebank AK315577) were cloned by PCR from 293T cell cDNA (TA cloning kit, Invitrogen, Carlsbad, CA, USA) using the following primers: 5′-AAAGGTGCTCCGCCGCTAAG-3′ (hVAPB sense), 5′-TTCTTTTCCCCCTCAATCAG-3′ (hVAPB antisense), 5′-CCGATGGCGTCCGCCTCAGGGGCC-3′ (hVAPA sense) and 5′-CTACAAGATGAATTTCCCTAG-3′ (hVAPA antisense). To introduce P56S point mutation, site-directed mutagenesis was performed by PCR (QuickChange Site Directed Mutagenesis Kit, Stratagene, La Jolla, CA, USA) using $pCR2.1\text{-}hVAPB^{WT}$ as template and the following primer sequence: 5′-TGTGTGAGGTC-CAACAGCGGAATCA-3′ (sense). pUbc-enhanced green fluorescent protein (EGFP), $pUbc\text{-}hVAPB^{WT}$, $pUbc\text{-}hVAPB^{P56S}$ and pUbc-hVAPA were generated from the pCCL-cPPT-phosphoglycerokinase (PGK1)-WPRE expression vector (Raoul *et al.* 2005), in which PGK1 has been replaced by the human ubiquitin c promoter (Araki *et al.* 2004). To construct AAV vectors carrying EGFP, $hVAPB^{WT}$, $hVAPB^{P56S}$, hVAPA cDNA, we first replaced the cytomegalovirus promoter of pAAV-MCS (Stratagene) by the mouse PGK1 promoter (Raoul *et al.* 2005), and then cloned the corresponding cDNA downstream of PGK1 promoter and β-globin intron. All cDNA inserts were sequenced to ensure the integrity of the nucleotidic sequences.

AAV6 production and titration by quantitative real-time PCR

Recombinant AAV serotype 6 vectors were produced as previously described (Towne *et al.* 2008), by transient co-transfection of 293AAV cell line with AAV-EGFP, $AAV\text{-}hVAPB^{WT}$, $AAV\text{-}hVAPB^{P56S}$ or AAV-hVAPA and the helper plasmid pDF6 (Grimm *et al.* 2003). Forty-eight hours later, AAV particles were purified from cell lysates on a heparin affinity column using HPLC.

The titration of infectious AAV particles was performed in 293T cells by quantitative real-time PCR according to the nuclease S1 methods (Rohr *et al.* 2005), as previously described (Towne *et al.* 2008). The primers targeting β-globin intron were 5′-CGTGCCAA-GAGTGACGTAAG-3′ (sense) and 5′-TGGTGCAAAGAGGCAT-GATA-3′ (antisense). Albumin that served as internal control was amplified using the following primers: 5′- TGAAACATACGTTCC-CAAAGAGTTT-3′ (sense) and 5′-CTCTCCTTCTCAGAAAGTGT-GCATAT-3′ (antisense). The titers of AAV vectors used in the present study, depending on the viral preparation, vary between 2.1 and 2.9×10^{10} transducing units (TU)/mL for AAV-EGFP; 1.4 and 6.3×10^{9} TU/mL for $AAV\text{-}hVAPB^{WT}$; 1.8 and 2.5×10^{10} TU/mL for $AAV\text{-}hVAPB^{P56S}$; 2×10^{9} TU/mL for AAV-hVAPA.

Cell cultures

Motoneurons from E12.5 spinal cord of CD1 (Charles River Laboratories Inc., Wilmington, MA, USA) or *Hb9::GFP* (T.M. Jessell's laboratory, Columbia University, NY, USA) mice were isolated as described (Arce *et al.* 1999) and modified (Raoul *et al.* 2002) using iodixanol density gradient centrifugation. Motoneurons were plated on poly-ornithine/laminin-treated wells in the presence of a cocktail of neurotrophic factors (0.1 ng/mL glial-derived neurotrophic factor, 1 ng/mL brain-derived neurotrophic factor, and 10 ng/mL ciliary neurotrophic factor) in supplemented Neurobasal medium. Cortical and striatal neurons were isolated from E17.5 embryos as described (Raoul *et al.* 2002; Zala *et al.* 2005). Cortical and striatal neurons were plated on poly-ornithine/laminin-treated wells and cultured in Neurobasal medium complemented with 1 mM sodium pyruvate, 2% B27 supplement (Invitrogen). Housing and care of mice were performed in compliance with the European Community and National directives for the care and use of laboratory animals. Cos-7 and NSC34 cells were maintained in Dulbecco Modified Eagle Medium (Invitrogen) supplemented with 10% fetal bovine serum.

For infection of primary neurons, 1 day after plating, half of the culture media was removed and replaced with fresh supplemented media containing AAV particles. Cells were then incubated for 5 h at 37°C, washed and fed again with corresponding supplemented medium.

For survival assays we used the following reagents: tunicamycin, caffeine, dantrolene, 2,3-Dihydroxy-6-nitro-7-sulfamoyl-benzo (F) quinoxaline (NBQX) and MDL-28170 were from Sigma (St Louis, MO, USA). Thapsigargin and z-Asp(OMe)-Glu(OMe)-Val-Asp(OMe)-fmk were from Calbiochem (San Diego, CA, USA). Salubrinal and 1,2-*bis*(2-Aminophenoxy)ethane-N,N,N′,N′-tetraacetic acid tetrakis(acetoxymethyl) ester (BAPTA/AM) were from Alexis Corporation (San Diego, CA, USA). z-Ala-Thr-Ala-Asp(OME)-fmk (z-ATAD-fmk) was purchased from MBL international corporation (Woburn, MA, USA).

VAPB antibodies and Western blotting

Rabbit polyclonal antibodies for human VAPB (DIM-705) were raised using hVAPB peptide TVQSNSPISALAPTG conjugated to keyhole-limpet hemocyanin. Antisera were purified on peptide-sepharose affinity column (P.A.R.I.S, Compiègne, France).

Proteins were extracted using lysis buffer (50 mM Tris-HCl pH 7.5, 150 mM NaCl, 2 mM EDTA, 2 mM EGTA and 1% sodium dodecyl sulfate) supplemented with a protease inhibitor cocktail (Roche Molecular Biochemicals, Indianapolis, IN, USA). Protein concentration was determined using BCA kit (Pierce, Rockford, IL, USA). Protein samples were separated by sodium dodecyl sulfate–polyacrylamide gel electrophoresis and blotted to nitrocellulose membranes (Schleicher and Schuell, Whatman International Ltd, Springfield Mill, UK). All membrane blocking steps and antibody dilutions were performed with 6% non-fat dry milk in phosphate-buffered saline (PBS) containing 0.1% Tween-20, and washing steps performed with PBS containing 0.1% Tween-20. The following antibodies were used: anti-hVAPB (DIM-705, 1 : 4000), anti-VAPA (sc-48698, Santa Cruz Biotechnology, Santa Cruz, CA, USA; 1 : 1000), anti-EGFP (TP401, Torrey Pines Biolabs (East Orange, NJ, USA); 1 : 5000), anti-phospho inositol-requiring enzyme 1 (IRE1) (ab48187, Abcam (Cambridge, MA, USA); 1 : 200), anti-actin (AC-40; Sigma-Aldrich; 1 : 20 000). Proteins were then detected using horseradish peroxidase-conjugated secondary antibodies and visualized with the chemiluminescent horseradish peroxidase substrate (Millipore Corporation, Bedford, MA, USA).

Immunocytochemistry

Cells were cultured onto poly-ornithine/laminin-treated glass coverslips at a density of 5000 cells per cm^2 and at indicated times fixed in 3.7% formaldehyde for 20 min at 20°C. Cells were washed thrice with PBS and then blocked for 1 h in PBS, 0.1% Triton X-100, 4% bovine serum albumin and 5% heat-inactivated donkey serum. Coverslips were then incubated overnight at +4ºC with the appropriate antibody: anti-hVAPB (DIM-705; 1 : 500), anti-KDEL (Lys-Asp-Glu-Leu) (SPA-827, Stressgen, Collegeville, PA, USA; 1 : 500), anti-non-phosphorylated neurofilament (Covance, Princeton, NJ, USA); 1 : 500), anti-β-COP (M3A5, Sigma-Aldrich; 1 : 300), anti-GM130 (612008, BD Biosciences; 1 : 300), anti-cytochrome *c* (6H2.B4, BD Biosciences, Franklin Lakes, NJ, USA; 1 : 500), anti-phospho-IRE1 (ab48187, Abcam; 1 : 200), anti-cleaved caspase 3 (9661, Cell Signaling Technology, Beverly, MA, USA; 1 : 200), anti-caspase 12 (14F7, Sigma-Aldrich; 1 : 500). Cells were washed four times for 5 min each with PBS, incubated with the appropriate fluorescent-conjugated secondary antibody (Invitrogen), washed, and mounted in moviol.

For quantification of IRE1 phosphorylation, *Hb9::GFP* motoneurons were infected by indicated AAV and immunostained with anti-phospho-IRE1 antibodies as described above. Images of phospho-IRE1 immunostaining were collected with an Olympus (Tokyo, Japan) BX50WI confocal laser-scanning microscope using a 20× (UplanApo, N.A 0.70) objective. Fluorescence analysis was performed using Metamorph software (Universal Imaging Corporation, Downingtown, PA, USA) on *Hb9::GFP* motoneurons that were automatically selected on GFP native fluorescence. Analysis of mean fluorescence intensity was performed on 130-320 motoneurons per culture condition.

Calcium imaging

To monitor quantitative changes of $[Ca^{2+}]_i$ in *Hb9::GFP* motoneurons we used a Fura-Red acetoxymethyl ester (AM) dye (Invitrogen) whose emission spectra (630–700 nm) does not overlap with emission of GFP (500–600 nm) and thus allows effective ratiometric fluorescence measurement without any GFP emitted fluorescence contamination. Other ratiometric Ca^{2+}-sensitive dyes Indo-1 and fura-2 possess common with GFP emission spectra, partially overlap with GFP excitation spectra that introduces an additional mistake during quantitative ratiometric $[Ca^{2+}]_I$ measurements. For dye loading, coverlips were rinsed with an external solution containing 150 mM NaCl, 2 mM KCl, 2 mM $MgCl_2$, 2 mM $CaCl_2$, 10 mM HEPES, 10 mM glucose, pH 7.4 and incubated in the same solution containing 20 μM Fura-Red AM for 30 min in the dark at 20°C, the dye was washed off and the coverslips reincubated in the dark for a further 60 min at 20°C to allow de-esterification of the dye. After loading, coverslips were transferred to the stage of an NIKON Diaphot 300 microscope (20× or 40× long distance lens). To selectively visualize Ca^{2+}in motoneurons we first focused on GFP fluorescent cells using appropriate filter setting [excitation 480 (40) nm, emission 535 (50) nm] and thereafter acquired fluorescent images of Fura-Red. Fura-Red was alternately excited at 440 (10) nm and 490 (10) nm using a xenon light source (Sutter Instruments, Novato, CA, USA), and emission collected at 660 (50) nm using a CCD camera (Hamamatsu, Bridgewater, NJ, USA). All filters were bandpass with bandwidths indicated in parentheses (Chroma Technology corp., Bellows Falls, VT, USA). Images were acquired at 2 s intervals and analyzed offline with SimplePCI software (Hamamatsu). For $[Ca^{2+}]_I$ analysis we first draw regions of interest on motoneurons (GFP positive cells) and then applied these regions of interest for analysis of Fura-Red images. $[Ca^{2+}]_i$ values were presented as the 490/440 nm ratio. During experiments, neurons were continuously perfused with external solution. Twenty seconds after beginning the experiment neurons were activated by a brief (10 s) application of the solution containing 50 mM KCl (KCl replaced equimolar amount of NaCl in external solution and was applied via fast perfusion system).

Statistical analyses

Statistical analyses were performed by unpaired two-tailed *t* test or by a one-way analysis of variance (ANOVA) followed by a Student-Newman–Keuls's *post hoc* test using the GraphPad Instat software (GraphPad Software, La Jolla, CA, USA). Significance was accepted at the level of $p < 0.05$.

Results

AAV-mediated expression of hVAPB^{P56S} leads to the formation of cytoplasmic aggregates in embryonic motoneurons

To investigate the functional consequences of the expression of the ALS-linked human VAPB^{P56S} mutant (hVAPB^{P56S}) in motoneurons, we developed an *in vitro* model based on AAV-mediated gene transfer. Using a recombinant AAV serotype 6 driving expression of the enhanced green fluorescent protein (AAV-EGFP) (Fig. 1a), we showed that AAV provide a simple and efficient means of stable gene expression in the motoneuron culture system. Indeed, at the multiplicity of infection (m.o.i) of 10 TU per cell (3×10^4 TU/mL), AAV serotype 6 can transduce up to 90% of motoneurons, with an early and sustained transgene expression (detectable from 6 h to 15 days post-infection) and limited toxicity (Appendix S1).

Adeno-associated viral constructs were then engineered to achieve expression of human VAPB wild-type (AAV-hVAPB^{WT}), VAPB mutant (AAV-hVAPB^{P56S}) or hVAPA (AAV-hVAPA), a member of the VAP family, which has not been linked to motoneuron disease. To facilitate the detection of hVAPBs, we generated polyclonal antibodies that specifically recognize human VAPB, both in western blot and immunocytochemistry (Figure S1a–d). We confirmed by western blot the ability of AAV-hVAPB^{WT}, AAV-hVAPB^{P56S} and hVAPA viral vectors to drive expression of their corresponding transgene (Fig. 1b). In accordance with previous reports (Kanekura *et al.* 2006; Suzuki *et al.* 2009), we observed that steady-state levels of hVAPB^{P56S} were lower than that of hVAPB^{WT}, even though cells were infected with the same m.o.i. We next evaluated the cellular distribution of hVAPB^{WT}, hVAPB^{P56S} and hVAPA in motoneurons. Although, we showed functional AAV-mediated VAPA expression by western blot (Fig. 1b), we were not able, with the available antibodies, to specifically detect the human form of VAPA by immunofluorescence in motoneurons. We showed that hVAPB^{WT} co-localizes with KDEL, an ER marker and with β-COP a component of coat protein complex I vesicles in motoneurons (Fig. 1c–f). Whereas, AAV-mediated expression of hVAPB^{P56S} leads to the formation of cytoplasmic aggregates that frequently co-localized with KDEL and occasionally with β-COP (Fig. 1c–f), we did not observe any co-localization of hVAPB^{P56S} aggregates with the Golgi matrix protein GM130 or the mitochondrial marker, cytochrome *c* (Figure S2a and d). AAV are thus effective gene expression platforms to study the impact of hVAPB wild-type and mutant over-expression on motoneuron functional integrity.

Over-expression of hVAPB^{WT} and hVAPB^{P56S} selectively triggers death of motoneurons

We examined the consequence of the over-expression of VAP family members on motoneuron survival. After 24 h in culture, motoneurons were infected at the same m.o.i with AAV-hVAPB^{WT}, AAV-hVAPB^{P56S}, AAV-hVAPA or AAV-EGFP. According to the high-efficiency transduction of motoneurons by AAV, we directly counted, at the time indicated, the number of phase-bright neurons using morphological criteria as previously described (Raoul *et al.* 2002). Regardless of the inherent toxicity of viral vectors (Appendix S1), the survival curves of motoneurons infected with AAV-hVAPA or AAV-EGFP motoneuron did not significantly vary over the time and were indistinguishable (Fig. 2a). In contrast, AAV-mediated expression of hVAPB^{WT} induced rapid death of motoneurons, half of them dying by 1 day post-infection (DPI). Expression of hVAPB^{WT} for a longer period (4 DPI) did not result in any further increase in cell death, even though expression of hVAPB^{WT} continued in the surviving motoneurons (not shown). Interestingly, we observed that motoneurons infected with the disease-associated hVAPB^{P56S} died more slowly than neurons infected with wild-type hVAPB (Fig. 2a). It is noteworthy that the susceptibility of motoneurons to hVAPB^{P56S} may not necessarily correlate with the presence of cytoplasmic inclusions. Indeed, at 2, 3 or 4 DPI, the surviving motoneurons showed an accumulation of hVAPB^{P56S} into cytoplasmic aggregates (Fig. 1c–f and not shown).

To establish whether the vulnerability of motoneurons to hVAPBs over-expression might be relevant to pathogenesis of motoneuron disease, we determined the susceptibility of other neuronal types to hVAPB^{WT} or hVAPB^{P56S} over-expression. We first evaluated the efficacy of AAV6 to drive transgene expression in embryonic cortical and striatal neurons. We showed that 92.1 ± 1.9% of cortical and 91.3 ± 2.1% of striatal neurons were transduced by AAV-EGFP (mean ± SD, $n = 3$). The toxicity associated with AAV vectors was 14.9 ± 1.8% for cortical neurons and 18.6 ± 5.2% for striatal neurons (mean ± SD, $n = 3$). When both types of neurons were infected with AAV-hVAPB^{WT} and AAV-hVAPB^{P56S}, we observed the expression of hVAPB^{WT} in the ER and the accumulation of hVAPB^{P56S} as cytoplasmic aggregates (Figure S3a and b). We then analyzed the time-dependent survival of cortical and striatal neurons infected with AAV-hVAPB^{WT}, AAV-hVAPB^{P56S}, AAV-hVAPA or AAV-EGFP. Contrary to motoneurons, we found that the survival of cortical and striatal neurons infected with AAV-hVAPB^{WT} and AAV-hVAPB^{P56S} was similar to the survival of those infected with AAV-hVAPA and AAV-EGFP viral vectors (Fig. 2b and c). These findings indicate that motoneurons are selectively vulnerable to increased levels of both wild-type and mutant VAPB.

AAV-based expression of hVAPB^{WT} and hVAPB^{P56S} induces ER stress in motoneurons

Three proximal sensors in mammalian cells trigger ER stress response: the IRE1, the double-stranded RNA-activated

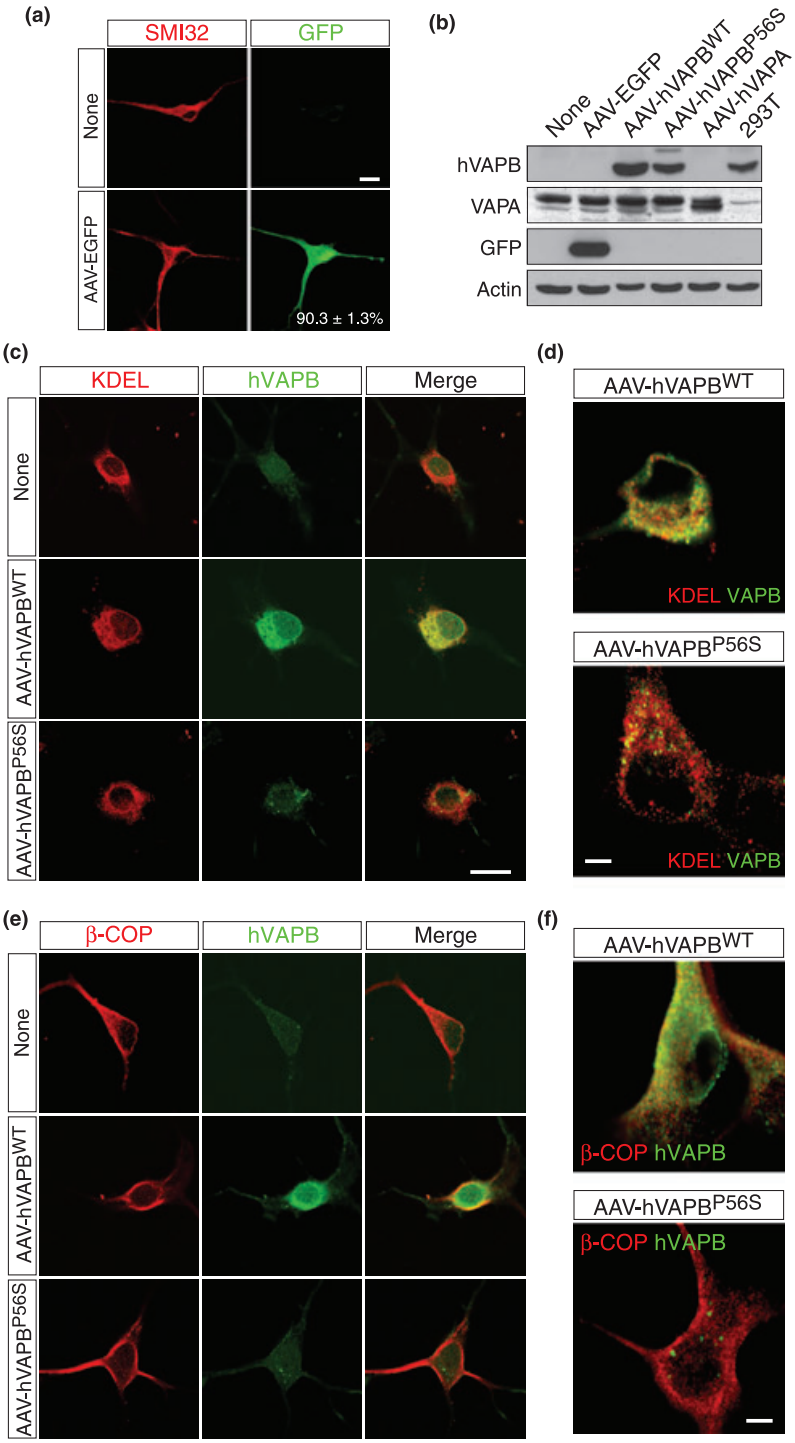

Fig. 1 Human vesicle-associated membrane protein-associated protein B wild-type (hVAPB^{WT}) mainly localizes at the ER, whereas mutated hVAPB (hVAPB^{P56S}) forms cytosolic aggregates in Adeno-associated viral (AAV)-transduced motoneurons. (a) EGFP fluorescence in motoneurons, as identified by non-phosphorylated neurofilament (SMI32) immunostaining, 2 days following infection with AAV-EGFP. AAV serotype 6 transduce up to 90% of motoneurons *in vitro*. (b) Western Blot analysis of hVAPB, hVAPA and EGFP expression in NSC34 cells 2 days post-infection (DPI). The actin was used as a loading control. To study hVAPB^{WT} and hVAPB^{P56S} subcellular localization, motoneurons were infected (or not) with AAV-hVAPB^{WT} or AAV-hVAPB^{P56S} and processed for co-immunostaining with anti-hVAPB and anti-KDEL (c, d) or anti-β-COP antibodies (e, f) 1 DPI for hVAPB^{WT} and 3 DPI for hVAPB^{P56S} [the time at which VAPB mutant aggregate become obvious]. (d) and (f) represent higher magnification images of motoneurons infected with AAV-hVAPB^{WT} and AAV-hVAPB^{P56S}, co-immunostained with hVAPB and KDEL (d) or β-COP (f). Scale bar in (c) and (e), 20 μm; (d) and (f), 2 μm.

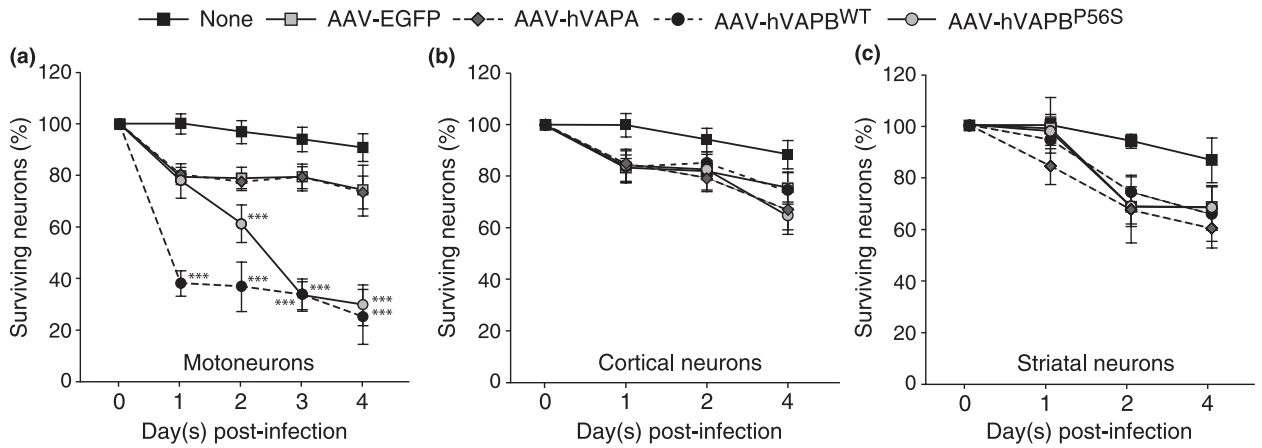

Fig. 2 Adeno-associated viral (AAV)-mediated expression of human vesicle-associated membrane protein-associated protein B wild-type (hVAPB^{WT}) and hVAPB^{P56S} selectively induces death of motoneurons. Motoneurons (a), cortical (b) and striatal (c) neurons were plated at the density of 1500 cells per cm^2, cultured for 1 day and infected with indicated AAV vectors at the multiplicity of infection of 10 transducing units per cell. The number of surviving neurons was determined at indicated times by counting cells under phase-contrast microscope. Neuron survival was expressed as a percentage of the number of surviving neurons in non-infected conditions for each day. Data represent the mean values ± SD of three independent experiments, each performed in triplicate or quadruplicate (ANOVA with Student-Newman–Keuls's *post hoc* test, ***$p < 0.001$).

protein kinase-like ER kinase1 and the protein activating transcription factor 6 (ATF6). VAPB has been proposed to act in the ER stress response. Nevertheless, how VAPB contributes to the homeostatic response of ER to stress remains unclear. Indeed, over-expression of VAPB wild-type but not VAPB mutant, triggered activation of the IRE1 downstream effector, X-box binding protein (XBP1) in NSC34 cell line (Kanekura *et al.* 2006; Suzuki *et al.* 2009). In another study, over-expression of both wild-type and mutant VAPB attenuated ATF6/XBP1-dependent transcription in HEK293 and NSC34 cells (Gkogkas *et al.* 2008). We therefore explored whether ER stress might contribute to the vulnerability of primary motoneurons to hVAPBs over-expression. Toward this goal, we determined by quantitative confocal microscopy the phosphorylation status of IRE1 in motoneurons. To identify motoneurons in an automated manner, we isolated them from *Hb9::GFP* mice in which, the motoneuron-selective *Hb9* promoter drives expression of the GFP (Wichterle *et al.* 2002). After validating the specificity of phospho-IRE1 immunoreactivity (Figure S4), we revealed that the ER stress inducer thapsigargin, induced an IRE1-dependent ER stress response in *Hb9::GFP* motoneurons (Fig. 3a and b). As activation of IRE1 is an early key event in ER stress, we analyzed the phosphorylation levels of IRE1 6 h post-infection. As mentioned above, at this early time point, any native EGFP, that might interfere in the automated identification of *Hb9::GFP* motoneurons was not observed in normal neurons infected with AAV-EGFP. When motoneurons were infected both with AAV-hVAPB^{WT} and AAV-hVAPB^{P56S}, we found a significant increase in the immunofluorescence intensities of phosphorylated IRE1 (Fig. 3b). In contrast, the mean phospho-IRE1 immunofluorescence of motoneurons infected with AAV-EGFP did not differ from that of non-infected cells (Fig. 3b).

Salubrinal can act as a neuroprotective agent through inhibition of ER stress (Saxena *et al.* 2009). When added to culture media, we found that salubrinal saved motoneurons from death induced by over-expression of both hVAPB^{WT} and hVAPB^{P56S} (Fig. 3c). We confirmed by counting the percentage of EGFP-positive motoneurons 4 DPI that salubrinal, at this concentration, did not lead to unspecific transcriptional or translational repression of the viral construct (AAV-EGFP-infected motoneurons, 100 ± 6.8%; AAV-EGFP-infected motoneurons treated with salubrinal, 94.1 ± 2.4% EGFP positive neurons at 4 DPI, mean ± SD, $n = 3$). These results suggest that ER stress is involved in death of motoneurons induced by over-expression of hVAPB^{WT} and hVAPB^{P56S}.

Motoneurons are more vulnerable than other neurons to an increase in intracellular Ca^{2+} levels

We next explored whether the ER stress pathway underlies the selective vulnerability of motoneurons to AAV-mediated over-expression of hVAPB^{WT} and hVAPB^{P56S}. Motoneurons, cortical and striatal neurons were thus challenged with increasing concentrations of the ER stress inducer tunicamycin, an inhibitor of *N*-glycosylation. Tunicamycin induces death of motoneurons, cortical and striatal neurons in a dose-dependent manner, and the dose response curve of motoneurons to tunicamycin did not significantly differ from that of cortical or striatal neurons (Fig. 4a). To confirm this result, we used thapsigargin, which induces ER stress by

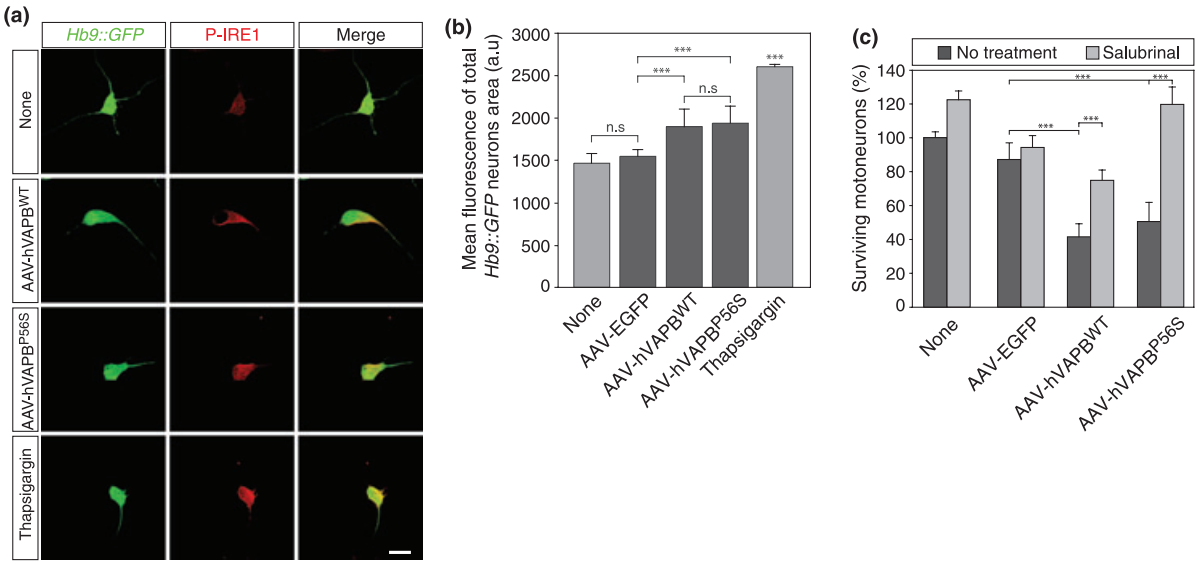

Fig. 3 Adeno-associated viral (AAV) 6-mediated over-expression of human vesicle-associated membrane protein-associated protein B wild-type (hVAPB^{WT}) and hVAPB^{P56S} induces ER stress activation in motoneurons. (a, b) Expression of both hVAPB^{WT} and hVAPB^{P56S} leads to increased levels of phosphorylated inositol-requiring enzyme 1 (IRE1) in motoneurons. (a) Immunodetection of phosphorylated IRE1 in motoneurons isolated from *Hb9::GFP* transgenic mice 6 h following infection with indicated viral vectors. Scale bar, 20 μm. (b) Quantification of phospho-IRE1 fluorescence in *Hb9::GFP* motoneurons infected (or not) with AAV-EGFP, AAV-hVAPB^{WT} or AAV-hVAPB^{P56S}. Confocal fluorescence imaging and Metamorph image analysis were used to determine mean fluorescence intensity in indicated conditions (a.u, arbitrary unit). (c) Salubrinal saves motoneurons from hVAPB-induced death. Motoneurons were infected with indicated viral vectors and cultured in the presence or absence of salubrinal (5 μM). Survival was determined at 4 day post-infection. Motoneuron survival was expressed relative to non-infected neurons in the presence or not of salubrinal. Results shown in (b) and (c) are the mean values ± SD of three independent experiments performed in triplicates (ANOVA with Student-Newman–Keuls's *post hoc* test, ***$p < 0.001$; n.s, non-significant).

disrupting intralumenal Ca^{2+} homeostasis through a selective inhibition of the sarco/endoplasmic reticulum Ca^{2+} ATPase. Interestingly, we observed that motoneurons show an increased susceptibility to thapsigargin-induced ER stress compared to cortical and striatal neurons (Fig. 4b). This suggests that motoneurons might have an exacerbated susceptibility to aberrant Ca^{2+} signals rather than to ER stress. With this in mind, we cultured motoneurons, cortical and striatal neurons in the presence of increasing concentrations of caffeine, an agonist of ryanodine receptors (RyRs) driving release of Ca^{2+} from the ER. Caffeine does not significantly affect survival of cortical and striatal neurons, whereas under the same conditions, caffeine induces death of about 50% of motoneurons in a dose-dependent manner (Fig. 4c). Overall our findings suggest that despite the involvement of the ER stress response in the death of motoneurons induced by hVAPB^{WT} and hVAPB^{P56S} over-expression, an altered Ca^{2+} homeostasis might underlie their selective vulnerability.

AAV-mediated over-expression of wild-type and mutant human VAPB impairs Ca^{2+} homeostasis in motoneurons

To investigate whether the over-expression of hVAPB^{WT} or hVAPB^{P56S} has an impact on the capacity of Ca^{2+} regulation in motoneurons, we examined through ratiometric Ca^{2+} imaging their responses to a high potassium (K^+) stimulus. Indeed, high K^+ depolarization evokes a Ca^{2+} influx, whose amplitude depends on the homeostatic regulation of intracellular Ca^{2+} [$(Ca^{2+})_i$](Gou-Fabregas *et al.* 2009). To facilitate the analysis of Ca^{2+} transients in motoneurons, we isolated them from *Hb9::GFP* transgenic mice. Simultaneous dual-color imaging of GFP and the Ca^{2+}-sensitive dyes Fura-Red was performed 6 h post-infection to study early events taking place well before the resulting cell death (Fig. 5a). At this time point, we were not able to detect any native EGFP fluorescence in AAV-EGFP-infected motoneurons that might interfere in the identification of *Hb9::GFP* motoneurons. We first showed that motoneurons, infected or not, respond to membrane depolarization by a Ca^{2+} influx that leads to an increased $[Ca^{2+}]_i$ (Fig. 5a–c). It is noteworthy that a trend (non-significant) towards greater basal Ca^{2+} levels in motoneurons was seen following transduction with hVAPB^{WT} and hVAPB^{P56S} compared to EGFP (Fig. 5d). When we determined the amplitude of the Ca^{2+} response to high K^+ concentrations, we found that AAV-mediated expression of both hVAPB^{WT} and hVAPB^{P56S} led to a significant reduction in the amplitude of Ca^{2+} transients (Fig. 5e). This suggests that death of motoneurons, induced by over-expression of

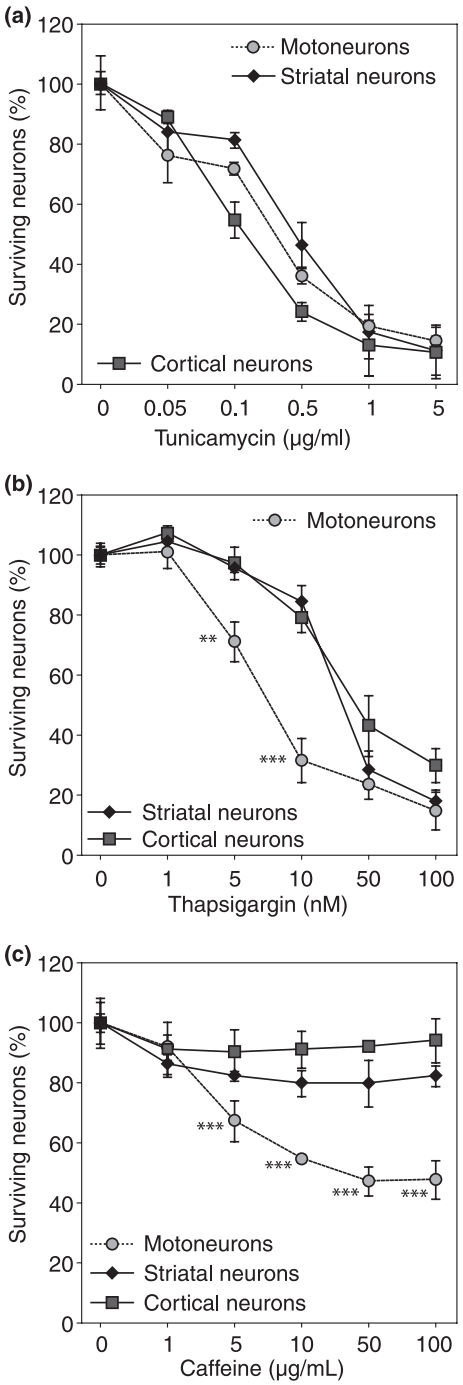

Fig. 4 Motoneurons show an increased susceptibility to calcium release from the ER. Motoneurons, cortical and striatal neurons were cultured for 1 day, treated with indicated concentrations of thapsigargin (a), caffeine (b) and tunycamycin (c) and survival determined by direct counting 1 day after. Neuron survival was expressed relative to the number of cells surviving in the non-treated condition. Data represent the mean values ± SD of three independent experiments (ANOVA with Student-Newman–Keuls's *post hoc* test, $^{**}p < 0.01$, $^{***}p < 0.001$).

wild-type and mutant hVAPB, might rely on changes in the intracellular calcium homeostasis.

Ca^{2+} signals are required to trigger death of motoneurons following over-expression of wild-type and mutant hVAPB

We next aimed at investigating the functional contribution of Ca^{2+} in motoneuron death induced by over-expression of $hVAPB^{WT}$ or $hVAPB^{P56S}$. We first examined the effect of the reduction of $[Ca^{2+}]_i$ on motoneuron survival by using the membrane permeable Ca^{2+} chelator BAPTA/AM. We found that BAPTA/AM prevented motoneuron death following infection with AAV-$hVAPB^{WT}$ and $hVAPB^{P56S}$ (Fig. 6a and Figure S5a), arguing for a role of Ca^{2+} signals in the death process.

The selective sensitivity of motoneurons to an elevation of $[Ca^{2+}]_i$ through activation of RyRs (Fig. 4c) paralleled the disturbed Ca^{2+} homeostasis associated with $hVAPB^{WT}$ and $hVAPB^{P56S}$ over-expression (Fig. 5e), suggests that Ca^{2+} signals from the ER store may intervene in the death pathway. We then evaluated the neuroprotective effect of dantrolene, a selective inhibitor of RyRs that antagonizes Ca^{2+}-induced Ca^{2+} release (CICR), on hVAPB-induced death. We first ensured that dantrolene did not unspecifically influence viral-mediated gene expression in motoneurons (AAV-EGFP, 100 ± 2.4%; AAV-EGFP with dantrolene, 94 ± 6.8% EGFP positive motoneurons at 4 DPI, mean ± SD, $n = 3$). We then showed that dantrolene significantly saved motoneurons from AAV-mediated over-expression of $hVAPB^{WT}$ and $hVAPB^{P56S}$ (Fig. 6b and Figure S5b), suggesting that activation of CICR via RyRs participates in Ca^{2+}-dependent death signaling in motoneurons.

Ca^{2+}-induced Ca^{2+} release has been demonstrated to participate in the generation of Ca^{2+} transients elicited by α-amino-3-hydroxy-5-methylisoxazole-4-propionate (AMPA)/Kainate (KA)-type glutamate receptors during spontaneously occurring excitatory post-synaptic currents in cultured motoneurons (Jahn *et al.* 2006). Thus, we hypothesized that the impaired homeostatic regulation of Ca^{2+} induced by $hVAPB^{WT}$ and $hVAPB^{P56S}$ would impact on survival through an aberrant response to AMPA/KA-mediated Ca^{2+} influxes evoked by spontaneous inward currents. To address this question, we determined whether the AMPA/KA antagonist, NBQX, protected motoneurons from $hVAPB^{WT}$ and $hVAPB^{P56S}$ over-expression. As predicted, exposing motoneurons infected with AAV-$hVAPB^{WT}$ and AAV-$hVAPB^{P56S}$ to NBQX, significantly rescues them from the degenerative process (Fig. 6c and Figure S5c). We checked that NBQX did not lead to an unspecific repression of viral-mediated gene expression (AAV-EGFP, 100 ± 7.9%; AAV-EGFP in the presence of NBQX, 93.6 ± 8.1% EGFP positive motoneurons at 4 DPI, mean ± SD, $n = 3$). Collectively, our results suggest that defective Ca^{2+} signaling contributes to the death of motoneurons induced by the over-expression of $hVAPB^{WT}$ and $hVAPB^{P56S}$.

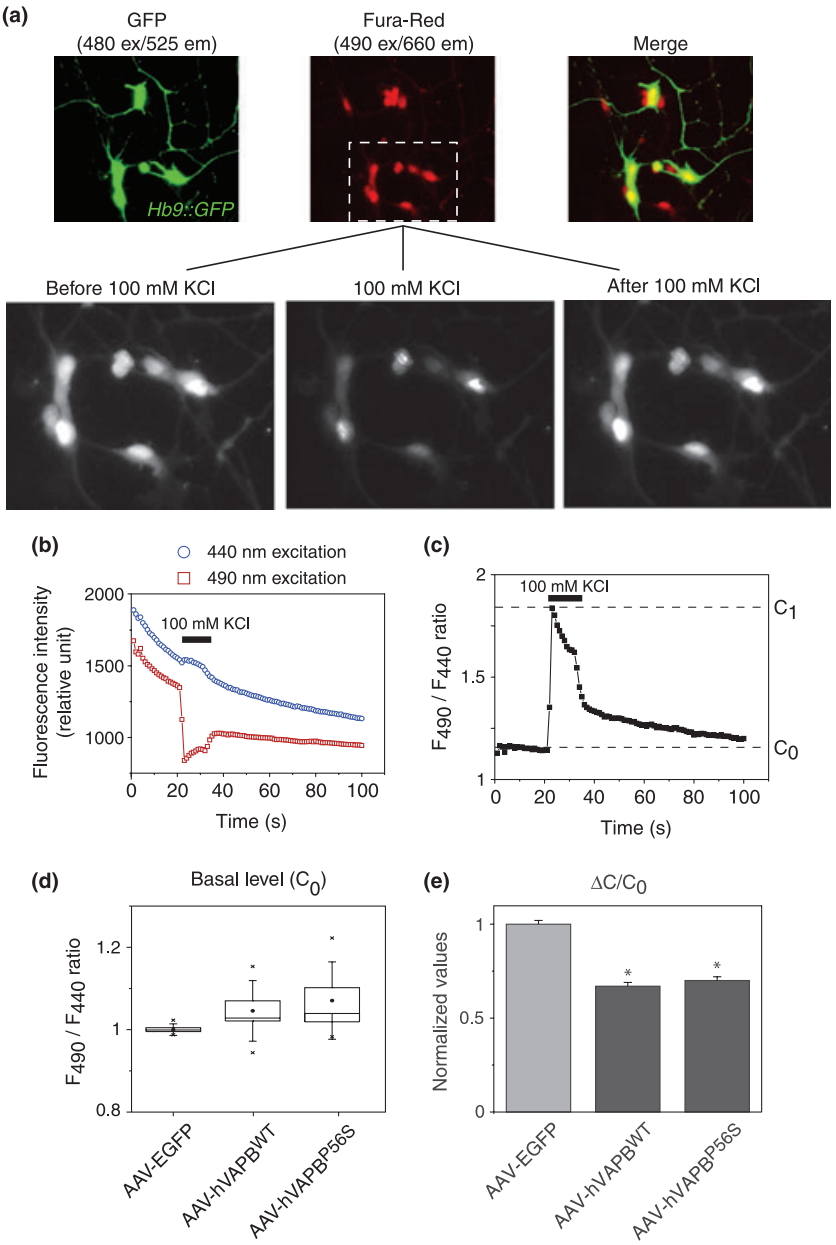

Fig. 5 Adeno-associated viral (AAV) 6-mediated over-expression of human vesicle-associated membrane protein-associated protein B wild-type (hVAPB^{WT}) and hVAPB^{P56S} disturbs calcium homeostasis in motoneurons. (a) Ratiometric $[Ca^{2+}]_i$ measurement in motoneurons. Top row represents an example of GFP and Fura-Red fluorescences in the same *Hb9::GFP* motoneurons (taken using mentioned filter sets, see materials and methods). The equal intensity of Fura-Red fluorescence in both GFP positive and GFP negative cells (top right image) highlights the absence of overlap between GFP and Fura-Red fluorescence signals. Bottom row represents Fura-Red fluorescence (excitation 490 nm) in neurons before, during and after bath application of 100 mM KCl. (b) $[Ca^{2+}]_i$ quantification in one of the motoneurons visualized in (a). Fura-Red fluorescence change when excited using 440 nm and 490 nm filters in response to KCl application. (c) Ratio of fluorescence intensities illustrated in (b). Basal level of $[Ca^{2+}]_i$ (d) and amplitudes of neuronal response to application of KCl (e) in motoneurons infected by indicated AAV. Data from five experiments, 10–20 neurons per experiment. Data shown in (d) are in box-and-whisker plot format and data in (e) are means ± SEM.

An ER-associated pathway is involved in death of motoneurons triggered by both hVAPB^{WT} and hVAPB^{P56S}

Which Ca^{2+}-dependent ER-related death executioners participate in motoneuron death following AAV-promoted over-expression of hVAPB^{WT} and hVAPB^{P56S}? The role of Ca^{2+}-activated cystein proteases, calpains, in neuronal death in response to Ca^{2+} signals has been well documented (Raynaud and Marcilhac 2006). To explore the functional

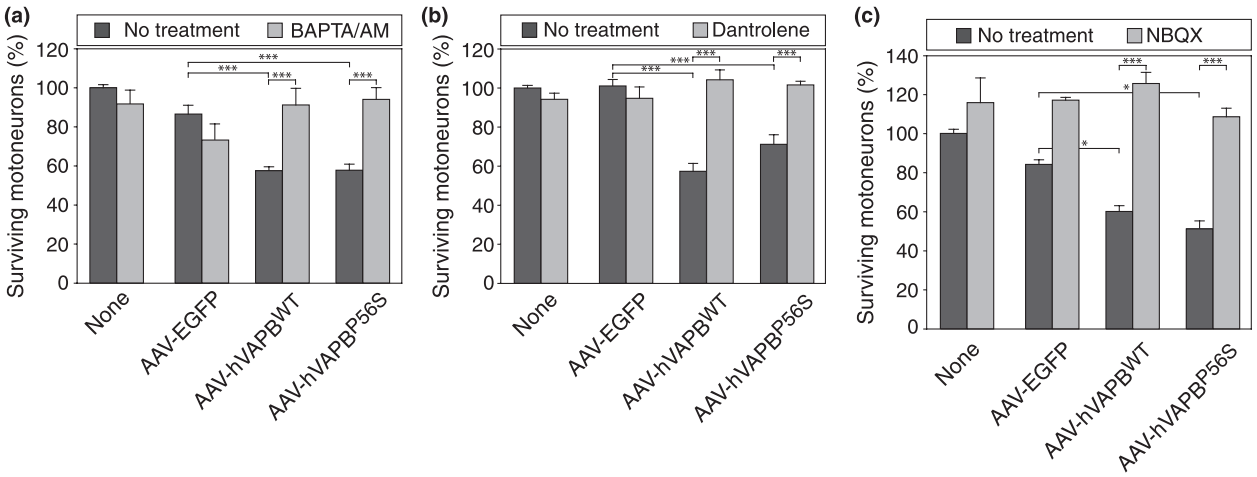

Fig. 6 Calcium signals are required for human vesicle-associated membrane protein-associated protein B (hVAPB)-induced death. Motoneurons were infected or not with Adeno-associated viral (AAV)-EGFP, AAV-hVAPB^{WT} or AAV-hVAPB^{P56S} 1 day after plating and treated or not with the intracellular Ca^{2+} chelator 1,2-*bis*(2-Aminophenoxy)ethane-N,N,N',N'-tetraacetic acid tetrakis(acetoxymethyl) ester (BAPTA/AM) (1 μg/mL) (a), the ryanodine receptors inhibitor dantrolene (5 μM) (b) or the α-amino-3-hydroxy-5-methylisoxazole-4-propionate/Kainate antagonist NBQX (10 μM) (c). Motoneuron survival was determined 4 day post-infection. All values are expressed as the mean ± SD of three independent experiments, each performed in triplicate (ANOVA with Student-Newman–Keuls's *post hoc* test, $^{*}p < 0.05$ and $^{***}p < 0.001$).

involvement of calpains in hVAPB-induced death, we used the potent inhibitor of the ubiquitously expressed μ- and m-calpain, MDL-28170 in our *in vitro* paradigm. We confirmed that at the indicated concentration MDL-28170 did not repress AAV-promoted transgene expression (AAV-EGFP, 100 ± 3%; AAV-EGFP in the presence of MDL-28170, 99.7 ± 5.1% EGFP positive motoneurons at 4 DPI, mean ± SD, $n = 3$). We subsequently found that treatment with MDL-28170 rescued AAV-hVAPB^{WT}- and AAV-hVAPB^{P56S}-infected motoneurons from death (Fig. 7a and Figure S5d).

Caspase 12 is an ER resident caspase that plays an important role during ER stress-induced apoptosis. In addition, caspase 12 can be proteolytically activated by calpains following an elevation of intracellular Ca^{2+} (Tan *et al.* 2006). We found that caspase 12 mainly co-localized with hVAPB^{WT} at the ER but barely co-localized with hVAPB mutant cytoplasmic aggregates in motoneurons (Figure S6a). When we irreversibly inhibited caspase 12 through the synthetic peptide z-ATAD-fmk, we saved motoneurons from death induced by over-expression of hVAPB^{WT} and hVAPB^{P56S} (Fig. 7b and Figure S6b). We also ensured that z-ATAD-fmk did not influence AAV-mediated transgene expression by determining the percentage of motoneurons showing EGFP fluorescence 4 DPI (AAV-EGFP, 100 ± 4.3%; AAV-EGFP in the presence of z-ATAD-fmk, 96.8 ± 6.1%, mean ± SD, $n = 3$). Our data suggests that caspase 12, in spite of its different co-localization with wild-type and mutant VAPB, is a common effector of the motoneuron death process.

Caspase 3 is the primary executioner caspase of the calpain-/caspase 12-dependent death pathway. To investigate whether caspase 3 contributed to hVAPB wild-type and mutant-induced death of motoneurons, we first probed motoneurons infected (or not) with AAV-EGFP, AAV-hVAPB^{WT} and hVAPB^{P56S} with antibodies specific to the cleaved form of caspase 3. Consistent with the kinetics of death promoted by hVAPB^{WT} and hVAPB^{P56S} over-expression, the percentage of motoneurons showing an activation of caspase 3 associated with a nuclear pyknosis increased more rapidly when neurons were transduced with hVAPB^{WT} (16 h post-infection), and more slowly when neurons were transduced with hVAPB^{P56S} (3 days post-infection) (Fig. 7c–e). To confirm the involvement of caspase 3 in the degenerative process *in vitro*, we employed the caspase 3/7 caspase inhibitor z-Asp(OMe)-Glu(OMe)-Val-Asp(OMe)-fmk, which saved motoneurons from death induced by hVAPB^{WT} and hVAPB^{P56S} over-expression (Fig. 7f and Figure S6c). All together, these results suggest that the death of motoneurons triggered by AAV-mediated over-expression of wild-type and mutant hVAPB implicates Ca^{2+} -sensitive calpains and an ER-associated caspase cascade.

Discussion

The results presented in this study are consistent with a causative role of P56S mutant VAPB in motoneuron degeneration (Nishimura *et al.* 2004, 2005). Here, we show that viral delivery of VAPB mutant selectively triggers death of cultured motoneurons. To our surprise, AAV-mediated over-expression of the wild-type form of VAPB, but not VAPA, also induces a selective death of motoneurons, with an even more rapid kinetics of death. The expression of hVAPB^{WT}

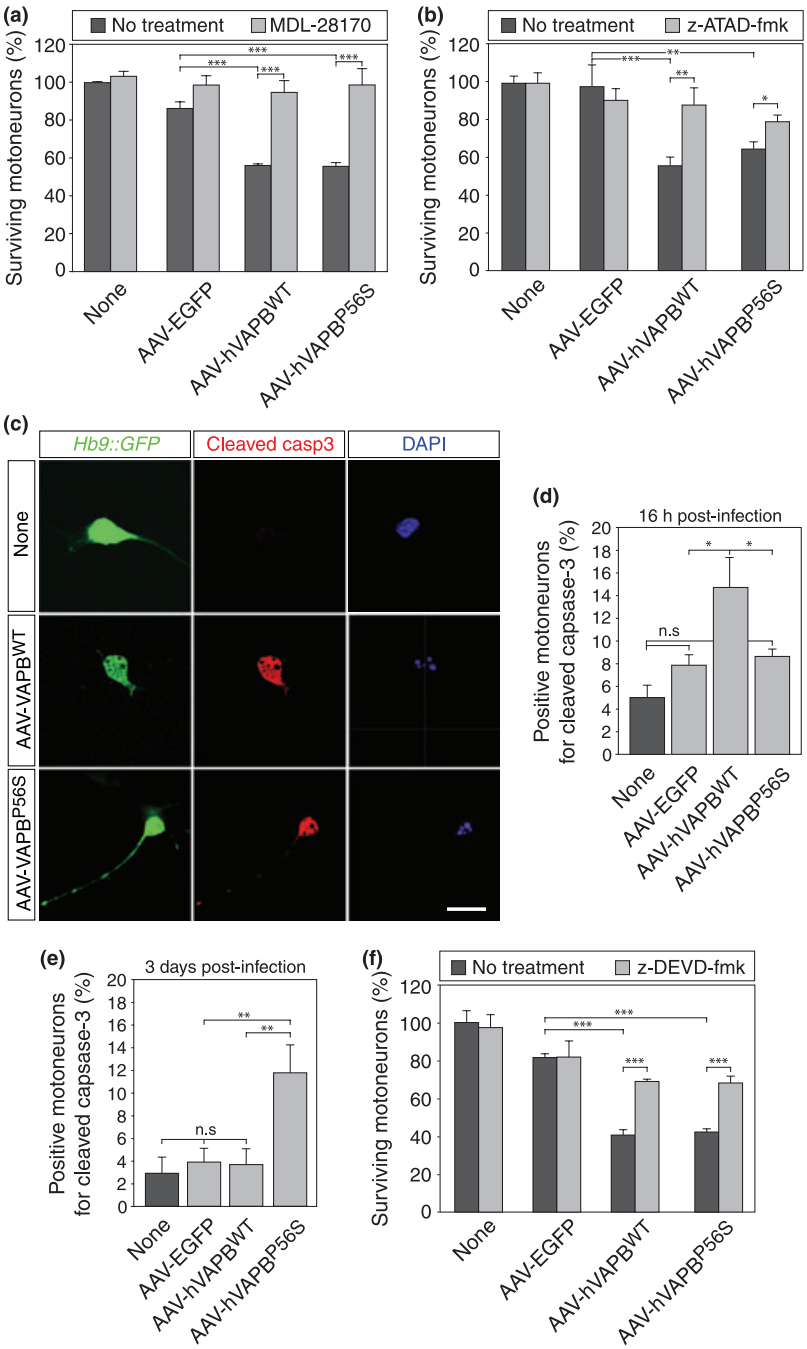

Fig. 7 Adeno-associated viral (AAV) 6-mediated over-expression of human vesicle-associated membrane protein-associated protein B wild-type (hVAPB^{WT}) and hVAPB^{P56S} triggers motoneuron death in a calpain and caspase-dependant manner. (a, b) Calpain and caspase 12 inhibitors save motoneurons from vesicle-associated membrane protein-associated protein B (VAPB)-induced death. Motoneurons were infected or not with indicated viral vectors and incubated in the presence or not of the calpain inhibitor MDL-28170 (5 μM) (a) or the caspase 12 inhibitor z-Ala-Thr-Ala-Asp(OME)-fmk (z-ATAD-fmk) (10 μM) (b). The number of surviving neurons in the presence or absence of the indicated inhibitor was expressed as a percentage of the number of non-infected surviving neurons 4 day post-infection. (c–e) Caspase 3 activation is involved in hVAPB^{WT} and hVAP^{P56S}-mediated death of motoneurons. *Hb9::GFP* motoneurons were infected or not with AAV-hVAPB^{WT} or AAV-VAPB^{P56S} and immunostained with antibodies directed against the cleaved form of caspase 3. The nuclei were stained with DAPI. (d, e) The percentage of motoneurons positive for cleaved caspase 3 and showing a pyknotic nucleus was determined 16 h (d) and 3 days (e) after the infection by indicated AAV. (f) Motoneuron survival was assessed 4 day post-infection with indicated AAV in the presence or not of the caspase 3 inhibitor z-Asp(OMe)-Glu(OMe)-Val-Asp(OMe)-fmk (z-DEVD-fmk; 10 μM). Graphs in (a), (b), (d), (e) and (f) show one representative of three independent experiments, (values are means ± SD, n.s, non-significant).

and hVAPB^{P56S} leads to ER stress, which contributes to the death process. However, the selective susceptibility of motoneurons to VAPBs over-expression compared to cortical and striatal neurons is most likely explained by an altered homeostatic regulation of Ca^{2+} signals. The implication of calpains, caspase 12 and caspase 3 completes this ER-associated Ca^{2+}-dependent death pathway induced by over-expression of both wild-type and mutant hVAPB.

The unfolded protein response (UPR) facilitates folding, processing, export, and degradation of proteins originating from the ER under stress conditions. When the stressful insult is too over-whelming, or when UPR is chronically activated, cells undergo apoptosis through a specific ER stress response (Schroder and Kaufman 2005). Recently, longitudinal gene expression profiling of ALS-vulnerable and ALS-resistant motoneurons in different SOD1 mutant models documented the critical role of ER stress in the selective susceptibility of motoneurons in the disease (Saxena *et al.* 2009). The accumulation of evidence that ER stress might also contribute to sporadic ALS, has highlighted the ER stress as an important physiopathologic mechanism in ALS (Ilieva *et al.* 2007; Atkin *et al.* 2008; Ito *et al.* 2009). Previous studies on the physiological involvement of VAPB in UPR and ER stress resulted in conflicting data as to whether VAPB^{WT} can induce or reduce the UPR. However, the P56S mutation that leads to the formation of aggregates and recruitment of the wild-type protein into these aggregates is most likely associated with a reduction of the activity of UPR in cell lines (Kanekura *et al.* 2006; Gkogkas *et al.* 2008; Suzuki *et al.* 2009). The negative impact of mutant VAPB on UPR activity may bring into play either a dominant negative effect that would block the VAPB-mediated activation of IRE1/XBP1 pathway (Kanekura *et al.* 2006; Suzuki *et al.* 2009) or potentiate the inhibitory activity of VAPB wild-type on ATF6 activation (Gkogkas *et al.* 2008). Here, we demonstrated that AAV delivery of both wild-type and mutated forms of VAPB led to activation of IRE1 (Fig. 3b) and that salubrinal, an ER-stress inhibitor that acts by preventing dephosphorylation of eukaryotic translation initiation factor-2 subunit-alpha, confered a neuroprotective effect (Boyce *et al.* 2005) (Fig. 3c). In addition, the specific inhibition of caspase 12, a representative caspase involved in ER stress, saved motoneurons from VAPBs over-expression (Fig. 7b and Figure S6b). Several factors may account for the discrepancies between our observations and those made by other studies. Firstly, viral gene transfer achieved a moderate gene expression level that may establish more physiological levels of expression. Secondly, we used non-tagged forms of VAPB proteins and it has been found that the nature and position of the tag sequence can influence the biochemical properties of the proteins (Suzuki *et al.* 2009). Perhaps more importantly, the use of primary motoneurons, displaying some intrinsic features of this neural cell type, may reveal more relevant pathogenic mechanisms.

It is striking that a proportion of motoneurons appeared intrinsically resistant to the over-expression both hVAPB^{WT} and hVAPB^{P56S} (Fig. 2a). This differential vulnerability of motoneurons to hVAPBs over-expression may reflect the diversity of intrinsic properties of motoneurons. Indeed, a variegation of intrinsic features has been proposed to underlie the selective vulnerability of motoneuron subtypes in the disease (Wetts and Vaughn 1996; Pun *et al.* 2006). In ALS mice, both ALS-resistant and ALS-vulnerable motoneurons show an early increase in ubiquitin signals, which might be regarded as a physiological response to mutant SOD1 misfolding. However, an activation of ER stress pathway selectively occurs in vulnerable subtypes (Saxena *et al.* 2009). Whether the motoneuron population sensitive to hVAPBs is the one that is more prone to ER stress response remains to be elucidated.

What might account for the selective vulnerability of motoneurons compared to other neuronal types? We observed a selective susceptibility of motoneurons to ER-stress induced by perturbed calcium homeostasis (Fig. 4b) compared to ER stress induced by accumulation of unfolded proteins (Fig. 4a), as well as a selective vulnerability of motoneurons to elevated $[Ca^{2+}]_i$ (Fig. 4c). This suggests that Ca^{2+} signals might determine an ER stress-mediated selective death of motoneurons. Several studies in SOD1 mutant FALS models propose that altered Ca^{2+} homeostasis underlies the selective vulnerability of motoneurons in ALS (von Lewinski and Keller 2005; Ionov 2007). ALS-vulnerable motoneurons in contrast to ALS-resistant and other neurons are characterized by low cytosolic Ca^{2+} buffering capacities (Vanselow and Keller 2000; von Lewinski *et al.* 2008). An increased Ca^{2+} permeability of the AMPA/KA receptors together with an impaired competence of Ca^{2+} clearance exacerbates glutamate-mediated excitatory neurotransmission, which may contribute to motoneuron vulnerability in ALS (Van Damme *et al.* 2005, 2007; Guatteo *et al.* 2007). Data obtained from ratiometric analysis of Ca^{2+} transients following membrane depolarization suggest that both wild-type and mutant forms alter the homeostatic regulation of Ca^{2+} (Fig. 5). Pharmacological inhibition of CICR, AMPA/KA receptors or Ca^{2+} -dependent calpain proteases, rescued hVAPB^{WT} and hVAPB^{P56S}-transduced motoneurons from death (Fig. 6). Collectively our data argue for a crucial role of Ca^{2+} signals in motoneuron vulnerability to hVAPB wild-type or mutant over-expression, and further delineate Ca^{2+} signals as an important pathological signal in motoneuron disease. Amplitude and duration of Ca^{2+} signals are determined by several interconnected mechanisms that control Ca^{2+} influx and extrusion through the plasma membrane as well as Ca^{2+} sequestration or release from intracellular stocks. How VAPB and its ALS-linked mutated form impact on this highly dynamic system remains to be elucidated.

Viral delivery of neurodegenerative disease-associated genes provides convenient models to investigate pathoge-

netic mechanisms *in vitro*. Cell-autonomous and non-cell-autonomous feature of motoneuron vulnerability in motoneuron disease has been investigated using primary or embryonic stem cell-derived culture of wild-type or SOD1 mutant motoneurons. For example, the selective vulnerability of motoneurons to AMPA-mediated excitotoxicity associated with GluR2 deficiency (Van Damme *et al.* 2007), the exacerbated susceptibility of motoneurons purified from SOD1 to the motoneuron-restricted Fas death pathway and its effector, the Collapsin Response Mediator Protein 4a (Raoul *et al.* 2002, 2006; Duplan *et al.* 2010), and the motoneuron-selective neurotoxic effects of SOD1 mutant damaged astrocytes (Pehar *et al.* 2004; Nagai *et al.* 2007). Importantly, these culture systems complement genetic *in vivo* models for studies of physiopathological mechanisms and are instrumental in the development of therapeutic strategies (Van Damme *et al.* 2005, 2007; Boillee *et al.* 2006; Locatelli *et al.* 2007; Yamanaka *et al.* 2008).

An important aspect of *in vitro* models relates to the etiological mechanisms underlying neurodegenerative diseases. Missense mutations in α-synuclein have been linked to autosomal dominant forms of Parkinson's disease. Experimental modeling of Parkinson's disease *in vitro* and *in vivo* through viral-based gene transfer approaches showed that over-expression of both the wild-type and mutant form of α-synuclein led to the death of dopaminergic neurons (Lo Bianco *et al.* 2002; Schneider *et al.* 2007). This suggests that increased endogenous levels of the wild-type protein can elicit neurotoxic effects in dopaminergic neurons in models. Interestingly, gene dosage effects resulting from the duplication or triplication of the α-synuclein gene was found to cause early-onset Parkinson's disease (Eriksen *et al.* 2005). Gene dosage effects were also reported in Alzheimer's disease, where the duplication of the amyloid precursor protein gene has been linked to early-onset Alzheimer's disease (Rovelet-Lecrux *et al.* 2006), and in the Charcot-Marie-Tooth type 1A motor sensory neuropathy, with duplication of the peripheral myelin protein 22 gene (Valentijn *et al.* 1992). Gene dosage effects, that have not yet been reported to cause ALS, might plausibly be another genetic factor in ALS.

Our data would indicate that the homeostatic function of VAPB within the ER is of a considerable biological significance in motoneurons. Abnormal expression levels of wild-type or expression of the mutated VAPB indeed led to the disregulation of ER homeostasis and resulted in motoneuron degeneration. A loss-of-function characterized by the aggregation of VAPB wild-type with or without other proteins has been hypothesized as the causal mechanism of ALS associated with P56S mutant VAPB (Kanekura *et al.* 2006; Teuling *et al.* 2007; Suzuki *et al.* 2009). The slower death kinetics observed following over-expression of VAPB mutant compared to wild-type VAPB could indeed result from a gradual depletion and subsequent loss-of-function of endogenous $VAPB^{WT}$. Unfortunately, rescue experiments consisting in the over-expression of wild-type protein in the presence of mutant protein cannot be achieved in our *in vitro* model. However, activation of the IRE1 signal and impaired Ca^{2+} homeostasis are early events that occur concomitantly following the forced expression of both $VAPB^{WT}$ and $hVAPB^{P56S}$. A plausible alternative hypothesis is that the mutant protein acquired one or more toxic properties that converge to the same effectors elicited when levels of the wild-type protein are abnormal. Much is yet to be understood about underlying mechanisms of the VAPB mutant protein in the degeneration of motoneurons. Genetic models of VAPB, including transgenic and VAPB-deficient mice will therefore be crucial for completing our understanding of motoneuron biology. Our *in vitro* model has helped us to identify potential effector mechanisms, which have been demonstrated relevant to other FALS models and therefore represent potential therapeutic targets for motoneuron disease.

Acknowledgements

We are indebted to Bernard Schneider, Vivianne Padrun and Fabienne Pidoux for their precious technical expertise. We specially thank Juan Iovanna for biosafety level 2 laboratory accommodation and François Michel for technical assistance with confocal microscopy. We are thankful to Brigitte Pettmann and Keith Dudley for their critical comments on earlier version of the manuscript; and to members of the Avenir team for support and discussion throughout this project. This work was supported by grants from the Institut National de la Santé et de la Recherche Médicale (Inserm), the American ALS association (ALSA), the Association Française contre les Myopathies (AFM), the Conseil Général des Bouches-du-Rhône and the Swiss National Science Foundation. K.L was a recipient of an Agence Nationale de la Recherche (ANR) grant.

Supporting information

Additional Supporting information may be found in the online version of this article:

Appendix S1. Supplementary Materials and methods.

Figure S1. DIM-705 rabbit polyclonal antibodies specifically recognize the human form of VAPB.

Figure S2. $hVAPB^{P56S}$ cyoplasmic aggregates do not colocalize with the golgi apparatus and mitochondria in motoneurons.

Figure S3. $hVAPB^{WT}$ localizes at the ER whereas $hVAPB^{P56S}$ forms cytosolic aggregates in cortical and striatal neurons.

Figure S4. Antibodies directed against the phosphorylated form of IRE1 specifically trace IRE1 activation following ER stress.

Figure S5. Short term protective effect of Ca^{2+} signaling inhibition against $hVAPB^{WT}$-induced death of motoneurons.

Figure S6. Inhibition of caspase 12 and 3 saves motoneurons from $hVAPB^{WT}$-induced death.

As a service to our authors and readers, this journal provides supporting information supplied by the authors. Such materials are peer-reviewed and may be re-organized for online delivery, but are

not copy-edited or typeset. Technical support issues arising from supporting information (other than missing files) should be addressed to the authors.

References

Amarilio R., Ramachandran S., Sabanay H. and Lev S. (2005) Differential regulation of endoplasmic reticulum structure through VAP-Nir protein interaction. *J. Biol. Chem.* **280**, 5934–5944.

Araki T., Sasaki Y. and Milbrandt J. (2004) Increased nuclear NAD biosynthesis and SIRT1 activation prevent axonal degeneration. *Science* **305**, 1010–1013.

Arce V., Garces A., de Bovis B., Filippi P., Henderson C., Pettmann B. and deLapeyriere O. (1999) Cardiotrophin-1 requires LIFRbeta to promote survival of mouse motoneurons purified by a novel technique. *J. Neurosci. Res.* **55**, 119–126.

Atkin J. D., Farg M. A., Walker A. K., McLean C., Tomas D. and Horne M. K. (2008) Endoplasmic reticulum stress and induction of the unfolded protein response in human sporadic amyotrophic lateral sclerosis. *Neurobiol. Dis.* **30**, 400–407.

Boillee S., Vande Velde C. and Cleveland D. W. (2006) ALS: a disease of motor neurons and their nonneuronal neighbors. *Neuron* **52**, 39–59.

Boyce M., Bryant K. F., Jousse C. *et al.* (2005) A selective inhibitor of eIF2alpha dephosphorylation protects cells from ER stress. *Science* **307**, 935–939.

Dimos J. T., Rodolfa K. T., Niakan K. K. *et al.* (2008) Induced pluripotent stem cells generated from patients with ALS can be differentiated into motor neurons. *Science* **321**, 1218–1221.

Dion P. A., Daoud H. and Rouleau G. A. (2009) Genetics of motor neuron disorders: new insights into pathogenic mechanisms. *Nat. Rev. Genet.* **10**, 769–782.

Duplan L., Bernard N., Casseron W. *et al.* (2010) Collapsin response mediator protein 4a (CRMP4a) is upregulated in motoneurons of mutant SOD1 mice and can trigger motoneuron axonal degeneration and cell death. *J. Neurosci.* **30**, 785–796.

Eriksen J. L., Przedborski S. and Petrucelli L. (2005) Gene dosage and pathogenesis of Parkinson's disease. *Trends Mol. Med.* **11**, 91–96.

Gkogkas C., Middleton S., Kremer A. M., Wardrope C., Hannah M., Gillingwater T. H. and Skehel P. (2008) VAPB interacts with and modulates the activity of ATF6. *Hum. Mol. Genet.* **17**, 1517–1526.

Gou-Fabregas M., Garcera A., Mincheva S., Perez-Garcia M. J., Comella J. X. and Soler R. M. (2009) Specific vulnerability of mouse spinal cord motoneurons to membrane depolarization. *J. Neurochem.* **110**, 1842–1854.

Grimm D., Kay M. A. and Kleinschmidt J. A. (2003) Helper virus-free, optically controllable, and two-plasmid-based production of adeno-associated virus vectors of serotypes 1 to 6. *Mol. Ther.* **7**, 839–850.

Guatteo E., Carunchio I., Pieri M., Albo F., Canu N., Mercuri N. B. and Zona C. (2007) Altered calcium homeostasis in motor neurons following AMPA receptor but not voltage-dependent calcium channels' activation in a genetic model of amyotrophic lateral sclerosis. *Neurobiol. Dis.* **28**, 90–100.

Ilieva E. V., Ayala V., Jove M. *et al.* (2007) Oxidative and endoplasmic reticulum stress interplay in sporadic amyotrophic lateral sclerosis. *Brain* **130**, 3111–3123.

Ionov I. D. (2007) Survey of ALS-associated factors potentially promoting Ca2+ overload of motor neurons. *Amyotroph. Lateral Scler.* **8**, 260–265.

Ito Y., Yamada M., Tanaka H. *et al.* (2009) Involvement of CHOP, an ER-stress apoptotic mediator, in both human sporadic ALS and ALS model mice. *Neurobiol. Dis.* **36**, 470–476.

Jahn K., Grosskreutz J., Haastert K., Ziegler E., Schlesinger F., Grothe C., Dengler R. and Bufler J. (2006) Temporospatial coupling of networked synaptic activation of AMPA-type glutamate receptor channels and calcium transients in cultured motoneurons. *Neuroscience* **142**, 1019–1029.

Kanekura K., Nishimoto I., Aiso S. and Matsuoka M. (2006) Characterization of amyotrophic lateral sclerosis-linked pro56ser mutation of vesicle-associated membrane protein-associated protein B (VAPB/ALS8). *J. Biol. Chem.* **281**, 30223–30233.

Lev S., Ben Halevy D., Peretti D. and Dahan N. (2008) The VAP protein family: from cellular functions to motor neuron disease. *Trends Cell Biol.* **18**, 282–290.

von Lewinski F. and Keller B. U. (2005) Ca2+, mitochondria and selective motoneuron vulnerability: implications for ALS. *Trends Neurosci.* **28**, 494–500.

von Lewinski F., Fuchs J., Vanselow B. K. and Keller B. U. (2008) Low Ca2+ buffering in hypoglossal motoneurons of mutant SOD1 (G93A) mice. *Neurosci. Lett.* **445**, 224–228.

Lo Bianco C., Ridet J. L., Schneider B. L., Deglon N. and Aebischer P. (2002) alpha-Synucleinopathy and selective dopaminergic neuron loss in a rat lentiviral-based model of Parkinson's disease. *Proc. Natl Acad. Sci. USA* **99**, 10813–10818.

Locatelli F., Corti S., Papadimitriou D. *et al.* (2007) Fas small interfering RNA reduces motoneuron death in amyotrophic lateral sclerosis mice. *Ann. Neurol.* **62**, 81–92.

Meininger V. (2005) Clinical trials in ALS: what did we learn from recent trials in humans? *Neurodegener. Dis.* **2**, 208–214.

Nagai M., Re D. B., Nagata T., Chalazonitis A., Jessell T. M., Wichterle H. and Przedborski S. (2007) Astrocytes expressing ALS-linked mutated SOD1 release factors selectively toxic to motor neurons. *Nat. Neurosci.* **10**, 615–622.

Nishimura A. L., Mitne-Neto M., Silva H. C. *et al.* (2004) A mutation in the vesicle-trafficking protein VAPB causes late-onset spinal muscular atrophy and amyotrophic lateral sclerosis. *Am. J. Hum. Genet.* **75**, 822–831.

Nishimura A. L., Al-Chalabi A. and Zatz M. (2005) A common founder for amyotrophic lateral sclerosis type 8 (ALS8) in the Brazilian population. *Hum. Genet.* **118**, 499–500.

Pehar M., Cassina P., Vargas M. R., Castellanos R., Viera L., Beckman J. S., Estevez A. G. and Barbeito L. (2004) Astrocytic production of nerve growth factor in motor neuron apoptosis: implications for amyotrophic lateral sclerosis. *J. Neurochem.* **89**, 464–473.

Peretti D., Dahan N., Shimoni E., Hirschberg K. and Lev S. (2008) Coordinated lipid transfer between the endoplasmic reticulum and the Golgi complex requires the VAP proteins and is essential for Golgi-mediated transport. *Mol. Biol. Cell* **19**, 3871–3884.

Prosser D. C., Tran D., Gougeon P. Y., Verly C. and Ngsee J. K. (2008) FFAT rescues VAPA-mediated inhibition of ER-to-Golgi transport and VAPB-mediated ER aggregation. *J. Cell Sci.* **121**, 3052–3061.

Pun S., Santos A. F., Saxena S., Xu L. and Caroni P. (2006) Selective vulnerability and pruning of phasic motoneuron axons in motoneuron disease alleviated by CNTF. *Nat. Neurosci.* **9**, 408–419.

Raoul C., Estevez A. G., Nishimune H., Cleveland D. W., deLapeyriere O., Henderson C. E., Haase G. and Pettmann B. (2002) Motoneuron death triggered by a specific pathway downstream of Fas. Potentiation by ALS-linked SOD1 mutations. *Neuron* **35**, 1067–1083.

Raoul C., Abbas-Terki T., Bensadoun J. C., Guillot S., Haase G., Szulc J., Henderson C. E. and Aebischer P. (2005) Lentiviral-mediated silencing of SOD1 through RNA interference retards disease onset and progression in a mouse model of ALS. *Nat. Med.* **11**, 423–428.

Raoul C., Buhler E., Sadeghi C., Jacquier A., Aebischer P., Pettmann B., Henderson C. E. and Haase G. (2006) Chronic activation in presymptomatic amyotrophic lateral sclerosis (ALS) mice of a feed-

back loop involving Fas, Daxx, and FasL. *Proc. Natl Acad. Sci. USA* **103**, 6007–6012.

Raynaud F. and Marcilhac A. (2006) Implication of calpain in neuronal apoptosis. A possible regulation of Alzheimer's disease. *FEBS J.* **273**, 3437–3443.

Rohr U. P., Heyd F., Neukirchen J. *et al.* (2005) Quantitative real-time PCR for titration of infectious recombinant AAV-2 particles. *J. Virol. Methods* **127**, 40–45.

Rovelet-Lecrux A., Hannequin D., Raux G. *et al.* (2006) APP locus duplication causes autosomal dominant early-onset Alzheimer disease with cerebral amyloid angiopathy. *Nat. Genet.* **38**, 24–26.

Saxena S., Cabuy E. and Caroni P. (2009) A role for motoneuron subtype-selective ER stress in disease manifestations of FALS mice. *Nat. Neurosci.* **12**, 627–636.

Schneider B. L., Seehus C. R., Capowski E. E., Aebischer P., Zhang S. C. and Svendsen C. N. (2007) Over-expression of alpha-synuclein in human neural progenitors leads to specific changes in fate and differentiation. *Hum. Mol. Genet.* **16**, 651–666.

Schroder M. and Kaufman R. J. (2005) The mammalian unfolded protein response. *Annu. Rev. Biochem.* **74**, 739–789.

Soussan L., Burakov D., Daniels M. P., Toister-Achituv M., Porat A., Yarden Y. and Elazar Z. (1999) ERG30, a VAP-33-related protein, functions in protein transport mediated by COPI vesicles. *J. Cell Biol.* **146**, 301–311.

Suzuki H., Kanekura K., Levine T. P., Kohno K., Olkkonen V. M., Aiso S. and Matsuoka M. (2009) ALS-linked P56S-VAPB, an aggregated loss-of-function mutant of VAPB, predisposes motor neurons to ER stress-related death by inducing aggregation of co-expressed wild-type VAPB. *J. Neurochem.* **108**, 973–985.

Tan Y., Dourdin N., Wu C., De Veyra T., Elce J. S. and Greer P. A. (2006) Ubiquitous calpains promote caspase 12 and JNK activation during endoplasmic reticulum stress-induced apoptosis. *J. Biol. Chem.* **281**, 16016–16024.

Teuling E., Ahmed S., Haasdijk E., Demmers J., Steinmetz M. O., Akhmanova A., Jaarsma D. and Hoogenraad C. C. (2007) Motor neuron disease-associated mutant vesicle-associated membrane protein-associated protein (VAP) B recruits wild-type VAPs into endoplasmic reticulum-derived tubular aggregates. *J. Neurosci.* **27**, 9801–9815.

Towne C., Raoul C., Schneider B. L. and Aebischer P. (2008) Systemic AAV6 delivery mediating RNA interference against SOD1: neuromuscular transduction does not alter disease progression in fALS mice. *Mol. Ther.* **16**, 1018–1025.

Turner B. J. and Talbot K. (2008) Transgenics, toxicity and therapeutics in rodent models of mutant SOD1-mediated familial ALS. *Prog. Neurobiol.* **85**, 94–134.

Valentijn L. J., Bolhuis P. A., Zorn I. *et al.* (1992) The peripheral myelin gene PMP-22/GAS-3 is duplicated in Charcot-Marie-Tooth disease type 1A. *Nat. Genet.* **1**, 166–170.

Van Damme P. and Robberecht W. (2009) Recent advances in motor neuron disease. *Curr. Opin. Neurol.* **22**, 486–492.

Van Damme P., Braeken D., Callewaert G., Robberecht W. and Van Den Bosch L. (2005) GluR2 deficiency accelerates motor neuron degeneration in a mouse model of amyotrophic lateral sclerosis. *J. Neuropathol. Exp. Neurol.* **64**, 605–612.

Van Damme P., Bogaert E., Dewil M. *et al.* (2007) Astrocytes regulate GluR2 expression in motor neurons and their vulnerability to excitotoxicity. *Proc. Natl Acad. Sci. USA* **104**, 14825–14830.

Vanselow B. K. and Keller B. U. (2000) Calcium dynamics and buffering in oculomotor neurones from mouse that are particularly resistant during amyotrophic lateral sclerosis (ALS)-related motoneurone disease. *J. Physiol.* **525**, 433–445.

Wegorzewska I., Bell S., Cairns N. J., Miller T. M. and Baloh R. H. (2009) TDP-43 mutant transgenic mice develop features of ALS and frontotemporal lobar degeneration. *Proc. Natl Acad. Sci. USA* **106**, 18809–18814.

Wetts R. and Vaughn J. E. (1996) Differential vulnerability of two subsets of spinal motor neurons in amyotrophic lateral sclerosis. *Exp. Neurol.* **141**, 248–255.

Wichterle H., Lieberam I., Porter J. A. and Jessell T. M. (2002) Directed differentiation of embryonic stem cells into motor neurons. *Cell* **110**, 385–397.

Yamanaka K., Chun S. J., Boillee S., Fujimori-Tonou N., Yamashita H., Gutmann D. H., Takahashi R., Misawa H. and Cleveland D. W. (2008) Astrocytes as determinants of disease progression in inherited amyotrophic lateral sclerosis. *Nat. Neurosci.* **11**, 251–253.

Zala D., Benchoua A., Brouillet E., Perrin V., Gaillard M. C., Zurn A. D., Aebischer P. and Deglon N. (2005) Progressive and selective striatal degeneration in primary neuronal cultures using lentiviral vector coding for a mutant huntingtin fragment. *Neurobiol. Dis.* **20**, 785–798.

